An enhanced core–shell interatomic potential for Te–O based oxides

Lyna Torzuoli, Assil Bouzid, Philippe Thomas, Olivier Masson

An enhanced core-shell interatomic potential for Te-O based oxides

Lyna Torzuoli, Assil Bouzid, Philippe Thomas and Olivier Masson

E-mail: assil.bouzid@unilim.fr
Institut de Recherche sur les Céramiques, UMR 7315 CNRS - Université de Limoges, Centre Européen de la Céramique, 12 rue Atlantis, 87068 Limoges Cedex, France.

Abstract. We present a new parametrization of the core-shell Buckingham interatomic potential (IAP) of Te-O oxides which allows to accurately reproduce experimental structural properties of various Te-O based systems including α-, β-, and γ-TeO_2. Based on this IAP, we generate high temperature model of TeO_2 and find that it features a liquid-like dynamical behaviour in contrast to previous models. Furthermore, we generate an amorphous TeO_2 model by quenching from the melt and study its structural properties in comparison with those available in the literature. We find that our model improves upon existent data and leads to a total pair correlation function in close agreement with the one measured through X-ray diffraction. These results open the way to systematic studies of binary and ternary complex Te-O based oxides by relying on a cheap, yet transferable and accurate IA potentials.

Submitted to: *Mater. Res. Express*

1. Introduction

TeO_2-based materials occurs either in crystalline or amorphous phases allowing for a wide range of applications encompassing photonics, optical devices, medical devices and telecommunications. [1, 2] In particular, TeO_2-based compounds find a high interest in telecommunication technologies thanks to their good linear and non-linear properties, low melting temperature (below 1000 °C) and large optical transmission window. [3] For exemple, their 3^{rd} order non linear susceptibilities are the highest among the known oxide glasses and reach 50 to 100 times higher than that of glassy SiO_2 [4] allowing for applications in Raman amplification [5, 6], ultra fast optical switches, and electro optic modulators [7, 8].

In spite of these outstanding properties, pure TeO_2 glass suffers from a low stability that requires the incorporation of modifier elements such as rare-earth atoms. This procedure allows one to tailor its mechanical properties, chemical stability window, refractive index, and optical response in order to target a given application. A better control of the macroscopic properties of binary and ternary TeO_2 based materials requires a deep understanding of their structural properties at the atomic scale. Hence, identifying the atomic scale origins of the measured properties will enable the design of efficient materials with desired properties. We note that TeO_2-based glasses were thoroughly investigated through several techniques including: x-ray diffraction [9, 10, 11], neutron diffraction [11, 12], NMR [13, 14, 15], EXAFS [16], and Raman scattering [17, 18, 19, 20, 21, 22]. While the experimental input to the atomic scale picture of TeO_2-based materials remains limited, modelling based on molecular dynamics simulations allows one to access the intimate details of the atomistic structures of this material. [23, 24, 25, 18, 26] In particular, classical molecular dynamics, based on empirical interatomic potentials, is an efficient tool to model the glassy structure at a low computational cost, while keeping a good accuracy.

The first TeO_2 interatomic potential (IAP) has been developed by Gulenko *et al.* [27] based on a core-shell Buckingham potential and allowed to model the structure of TeO_2. The resulting model fairly reproduced the lattice parameters of various crystalline TeO_2 phases as well as the experimental pair correlation function of glassy TeO_2. Nevertheless, at high temperatures the core-shell potential failed to converge and the authors had to use a rigid ion model and only include the shells at room temperature. While, the obtained amorphous model agrees well with experiments, it is of paramount importance to have a new parametrization of the IAP that allows one to properly simulate high temperature systems. Reproducing a correct dynamical behaviour of the investigated system is a prerequisite to model binary and ternary oxide glasses by relying on an unbiased parent high temperature model.

In this paper, we focus on modelling pure TeO_2 oxide through classical IAPs. First, we refine the core-shell Buckingham potential developed by Gulenko *et al.* [27] and reproduce the experimental lattice parameters of α-, β-, and γ-TeO_2 within less than 1% mean absolute error. Second, the obtained IAP is used to generate high temperature model of TeO_2 featuring a correct liquid-like dynamical properties. Finally, amorphous TeO_2 is generated by quenching from the melt. The obtained total pair correlation function shows a better agreement with experiments compared to that obtained in Ref. [27].

2. Refinement of the interatomic potential

2.1. Buckingham potential for crystalline TeO_2

In order to refine the IAP of TeO_2 we resort to the α-, β-, and γ- polymorphic structures of TeO_2. In the paratellurite form, or α-TeO_2, each tellurium atom is coordinated with four oxygen atoms forming TeO_4 disphenoids, with 2 equatorial bonds (1.879 Å) and two longer axial bonds (2.121 Å). The three-dimensional network is composed of corner-sharing TeO_2 disphenoids leading to asymmetric Te-$_{eq}$O$_{ax}$-Te bridges. [28] β-TeO_2 is the natural form of TeO_2. In this phase, each tellurium atom is coordinated with four oxygen atoms forming two equatorial bonds (1.877 and 1.927 Å) and two longer axial bonds (2.070 and 2.196 Å). The crystal lattice of β-TeO_2 has a layered structure with weakly bonded layers where the TeO_4 disphenoids share alternately corners and edges. In this polymorph, the tellirum atoms are connected *via* double bridges. [29] The last of the main polymorphs of TeO_2 is the metastable γ-TeO_2. This structure can be described with corner-sharing TeO_4 disphenoids, however, the disphenoids have a much more distorted geometry where one Te-O axial bond is longer than the other three (1.839 and 1.906 Å for the equatorial bonds and 2.048 and 2.241 Å for the axial bonds). Thus, the polyhedron is referred to as TeO_{3+1}. The chain-like network organization can be described as an infinite zigzag chain of TeO_3 units along the *c* axis. In this polymorph, one can distinguish two types of Te-O-Te bridges: highly asymmetric Te-$_{eq}$O(1)$_{ax}$-Te and nearly symmetric Te-$_{eq}$O(2)$_{ax}$-Te bridges. [30] Fitting these quite various structures ensures that our IAP will be efficient and transferable.

In practice, our theoretical procedure is based on the empirical IAPs within the Buckingham scheme for describing the short-range interaction as given by:

$$U_{ij}(r) = A_{ij}e^{-r/\rho_{ij}} - C_{ij}r^{-6} + \frac{q_i q_j}{4\pi\varepsilon_0}\frac{1}{r} \tag{1}$$

where A_{ij}, ρ_{ij} and C_{ij} are the Buckingham potential parameters, and q_i is the charge of ion i. Furthermore, we use a core-shell model to reproduce the polarisibilities of Te and O as given by:

$$U_{cs} = \frac{1}{2}k_2^{cs}x^2 + \frac{1}{24}k_4^{cs}x^4, \tag{2}$$

where *x* is the distance between the core and the shell. In this model, the shell and the core are coupled through a harmonic spring constant (k_2^{cs}) in the case of O. In the particular case of Te, it has been shown that adding an anharmonic term (k_4^{cs}) leads to a better description of its various asymmetric local environments in TeO_2-based oxides. [27] We start our potential refinement by considering the parameters (A_{ij}, ρ_{ij} and C_{ij}, k_2^{cs}, k_4^{cs} and q) of Ref. [27] and perform a simultaneous fit of the potential on 44 experimental observables including the atomic positions, lattice parameters and dielectric constants for α-, β-, γ-TeO_2 using the general utility lattice program (GULP) program. [31] This procedure differs from that of Ref. [27], where a sequential fit was performed on the crystalline phases of TeO_2. We here consider all three phases together and repeat the fitting until convergence of all potential parameters is

Table 1. Refined parameters of the Buckingham potential for the Te^{4+}–O^{2-} and O^{2-}–O^{2-} interactions and for the shell model for Te and O atoms. Values between parenthesis are the parameters from Ref. [27].

	A (eV)	ρ (Å)	C (eV.Å^6)
Buckingham potential			
Te_c^{4+}-O_{sh}^{2-}	1631.810731 (1595.266748)	0.346336 (0.345867)	0.020139 (1.0)
O_{sh}^{2-}-O_{sh}^{2-}	47902.536233 (82970.688434)	0.175930 (0.16099)	33.029759 (31.361954)
	k_2^{cs} (eV.Å^{-2})	k_4^{cs} (eV.Å^{-4})	q_s (e)
Shell model			
Te^{4+}	30.827429 (35.736418)	90.0 (90.0)	-1.975415
O^{2-}	61.600546 (61.776616)	0.0 (0.0)	-3.122581

Table 2. The calculated lattice parameters of α-TeO_2, β-TeO_2 and γ-TeO_2 compared to experiments [28, 29, 30] and previous modelling from PCCP 2014 [27]. The numbers between parenthesis represent the absolute error compared to experiments.

Parameter	Expt.	PCCP 2014 (error %)	This work (error %)
α-TeO_2	[28]		
a, b (Å)	4.810	4.831 (0.44)	4.841 (0.64)
c (Å)	7.613	7.349 (3.46)	7.498 (1.51)
Volume (Å^3)	176.135	171.548 (2.60)	175.692 (0.25)
α, β, γ	90.0	90.0 (0.0)	90.0 (0.0)
β-TeO_2	[29]		
a (Å)	12.035	11.550 (4.03)	12.090 (0.45)
b (Å)	5.464	5.473 (0.17)	5.482 (0.33)
c (Å)	5.607	5.549 (1.03)	5.559 (0.86)
Volume (Å^3)	368.712	350.814 (4.85)	368.449 (0.07)
α, β, γ	90.0	90.0 (0.0)	90.0 (0.0)
γ-TeO_2	[30]		
a (Å)	4.898	5.084 (3.79)	4.999 (2.06)
b (Å)	8.576	8.312 (3.08)	8.581 (0.06)
c (Å)	4.351	4.196 (3.55)	4.285 (1.51)
Volume (Å^3)	182.765	177.326 (2.98)	183.831 (0.58)
α, β, γ	90.0	90.0 (0.0)	90.0 (0.0)

reached. The final parameters are listed in table 1 and compared to the old parameters from Ref. [27].

Compared to the old potential [27], we here find smaller A (O-O) and C (Te-O) values which lead to a lower electronic and van der Waals interactions on the O-O and Te-O bonds, respectively. We note that k_4^{cs} is found to be insensitive to the fit. Consequently,

the experimental lattice parameters of crystalline TeO_2 are better reproduced with an overall mean absolute error of 0.9% compared to 2.2% obtained previously (see table 2).

2.2. Potential transferability

The transferability of the obtained IAP is checked against a large family of Tellurium oxides containing 13 TeO_2-based structures featuring different and various local environments around the Te atom. The obtained results are presented in table 3 and compared to experiments and to those obtained using the IAP of Ref. [27].

Table 3: The calculated lattice parameters of various TeO_2-based oxides compared to experiments and previous modelling from PCCP 2014 [27]. The numbers between parenthesis represent the absolute error compared to experiments.

Parameter	Expt.	PCCP 2014 (error %)	This work (error %)
$Ag_2Te_4O_{11}$	[32]		
a. (Å)	7.287	7.201 (1.19)	7.261 (0.35)
b. (Å)	7.388	7.304 (1.14)	7.332 (0.75)
c. (Å)	9.686	9.619 (0.69)	9.677 (0.09)
α	95.670	95.82 (0.16)	95.645 (0.03)
β	94.100	96.38 (2.42)	95.647 (1.64)
γ	119.400	119.50 (0.09)	119.356 (0.04)
$BaTe_2O_6$	[33]		
a. (Å)	5.569	5.5378 (0.56)	5.582 (0.22)
b. (Å)	12.796	13.285 (3.82)	13.266 (3.67)
c. (Å)	7.320	7.279 (0.55)	7.317 (0.04)
$\alpha.\ \beta.\ \gamma$	90.0	90.0 (0.0)	90.0 (0.0)
$Bi_2Te_4O_{11}$	[34]		
a. (Å)	6.991	6.797 (2.78)	6.818 (2.47)
b. (Å)	7.959	7.836 (1.55)	7.822 (1.72)
c. (Å)	18.896	18.299 (3.16)	18.390 (2.68)
$\alpha.\ \gamma$	90.0	90.0 (0.0)	90.0 (0.0)
β	95.176	93.049 (2.23)	93.557 (1.70)
$CaTe_2O_5$	[35]		
a. (Å)	9.382	9.376 (0.07)	9.434 (0.55)
b. (Å)	5.709	5.679 (0.53)	5.688 (0.38)
c. (Å)	11.132	11.055 (0.70)	11.081 (0.45)
$\alpha.\ \gamma$	90.0	90.0 (0.0)	90.0 (0.0)
β	115.109	114.764 (0.30)	115.710 (0.52)
$Co_6Te_5O_{16}$	[36]		
a. (Å)	11.032	11.146 (1.03)	11.188 (1.42)

Parameter	Expt.	PCCP 2014 (error %)	This work (error %)
b. (Å)	10.295	10.188 (1.04)	10.228 (0.65)
c. (Å)	12.876	12.807 (0.54)	12.851 (0.19)
$\alpha.\ \beta.\ \gamma$	90.0	90.0 (0.0)	90.0 (0.0)
$K_2Te_4O_{12}$	[37]		
a. (Å)	12.360	12.452 (0.74)	12.539 (1.45)
b. (Å)	7.248	7.189 (0.81)	7.240 (0.12)
c. (Å)	11.967	12.594 (5.24)	12.764 (6.66)
$\alpha.\ \gamma$	90.0	90.0 (0.0)	90.0 (0.0)
β	105.68	109.243 (3.37)	109.115 (3.25)
Li_2TeO_3	[38]		
a. (Å)	5.069	4.694 (7.39)	4.805 (5.21)
b. (Å)	9.566	9.811 (2.56)	9.770 (2.14)
c. (Å)	13.727	13.911 (1.34)	13.718 (0.07)
$\alpha.\ \gamma$	90.0	90.0 (0.0)	90.0 (0.0)
β	95.40	96.038 (0.67)	97.908 (2.63)
$MgTe_2O_5$	[39]		
a. (Å)	7.239	7.258 (0.26)	7.327 (1.21)
b. (Å)	10.658	10.614 (0.42)	10.734 (0.71)
c. (Å)	5.988	5.964 (0.40)	5.904 (1.41)
$\alpha.\ \beta.\ \gamma$	90.0	90.0 (0.0)	90.0 (0.0)
$Na_2Te_4O_9$	[40]		
a. (Å)	7.336	7.486 (2.04)	7.576 (3.27)
b. (Å)	10.449	10.750 (2.88)	10.788 (2.87)
c. (Å)	6.876	6.849 (0.40)	6.868 (0.12)
α	90.11	89.66 (0.50)	89.568 (0.60)
β	110.95	111.95 (0.90)	111.063 (0.10)
γ	69.52	69.47 (0.07)	69.978 (0.66)
Na_2TeO_3	[41]		
a. (Å)	6.882	7.017 (1.96)	6.975 (1.35)
b. (Å)	10.315	10.740 (4.12)	10.774 (4.45)
c. (Å)	4.961	4.873 (1.77)	4.902 (1.19)
$\alpha.\ \gamma$	90.0	90.0 (0.0)	90.0 (0.0)
β	91.66	91.938 (0.30)	92.807 (1.25)
$NiTe_2O_5$	[42]		
a. (Å)	8.868	8.448 (4.74)	8.407 (5.20)
b. (Å)	12.126	12.376 (2.06)	12.452 (2.69)
c. (Å)	8.452	8.451 (0.02)	8.619 (1.98)
$\alpha.\ \beta.\ \gamma$	90.0	90.0 (0.0)	90.0 (0.0)
$P_2Te_3O_{11}$	[43]		
a. (Å)	12.375	11.895 (3.88)	11.976 (3.22)
b. (Å)	7.317	7.077 (3.29)	7.160 (2.14)

Parameter	Expt.	PCCP 2014 (error %)	This work (error %)
c. (Å)	9.834	9.738 (0.98)	9.852 (0.18)
$\alpha.\ \gamma$	90.0	90.0 (0.0)	90.0 (0.0)
β	98.04	99.69 (1.68)	99.967 (1.97)
$SrTe_3O_8$	[44]		
a. b. (Å)	6.826	6.829 (0.06)	6.871 (0.66)
c. (Å)	6.760	6.636 (1.83)	6.667 (1.39)
$\alpha.\ \beta.\ \gamma$	90.0	90.0 (0.0)	90.0 (0.0)

Overall, our IAP reproduces the experimental lattice parameters of all the considered systems with a mean absolute error of 1.48%. These results validate the new parametrization of the IAP which can be now used to investigate the structures of Te-O disordered systems.

3. Liquid and Amorphous TeO_2

We resort to classical molecular dynamics simulations (MD) as implemented in the DL_POLY program [45] together with the obtained IAP to generate high temperature model of TeO_2. We consider a 768 atoms system (256 Te + 512 O) and 768 shells in a cubic box of side length 23.00 Å corresponding to the experimental density. [27] The temperature is controlled through a Berndson thermostat and a time step of 1 fs is used to integrate the equations of motion. The system has been equilibrated in the NVT ensemble for 60 ps at T=2100 K. For comparison, we also generate a second model based on the rigid-ion IAPs of Ref. [27]. Figure 1 shows the mean square displacement of Te and O as obtained from both models. We find that the new parametrization of the IAP leads to high mobility of both Te and O with a liquid-like diffusion coefficients amounting to 1.2 10^{-5} cm^2/ps and 3.3 10^{-5} cm^2/ps, respectively. However, in the case of the rigid-ion model the atomic mobility remains low even for simulation times reaching 150 ps and leads to diffusion coefficients one order of magnitude lower than the that obtained through the present parametrization (1.1 10^{-6} cm^2/ps and 6.2 10^{-6} cm^2/ps, for Te and O respectively). This result highlights the importance of including the shells when modelling oxides at high temperatures.

Next, we generate an amorphous TeO_2 model by gradually lowering the temperature to 1000 K, 600 K and 300 K. The system is equilibrated during 60 ps at each temperature plateau. Residual pressure effects are removed by further relaxing the glass at 300 K in the NPT ensemble for 500 ps yielding a slightly higher density (22.66 Å side length). Similarly, we produce a second amorphous system based in IAPs of Ref. [27] where the shells are only added at room temperature.

Figure 2 shows the total pair distribution function as obtained from our model and compared to experiments. Furthermore, we also display the results of the model generated using IAPs of Ref. [27]. We find that our new IAP model allows one to accurately reproduce the shape of the total pair correlation function measured experimentally. Compared to the previous model of Gulenko et al, our model reproduces slightly better the depth of the first minimum at 2.3 Å and the intensity of the peak at about 3.7 Å.

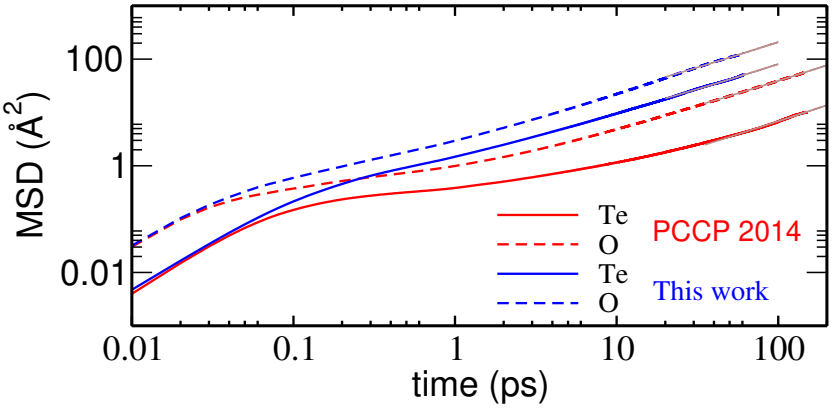

Figure 1. Mean square displacement as a function of the simulation time. The brown lines indicate the diffusive regime used to extract the diffusion coefficients.

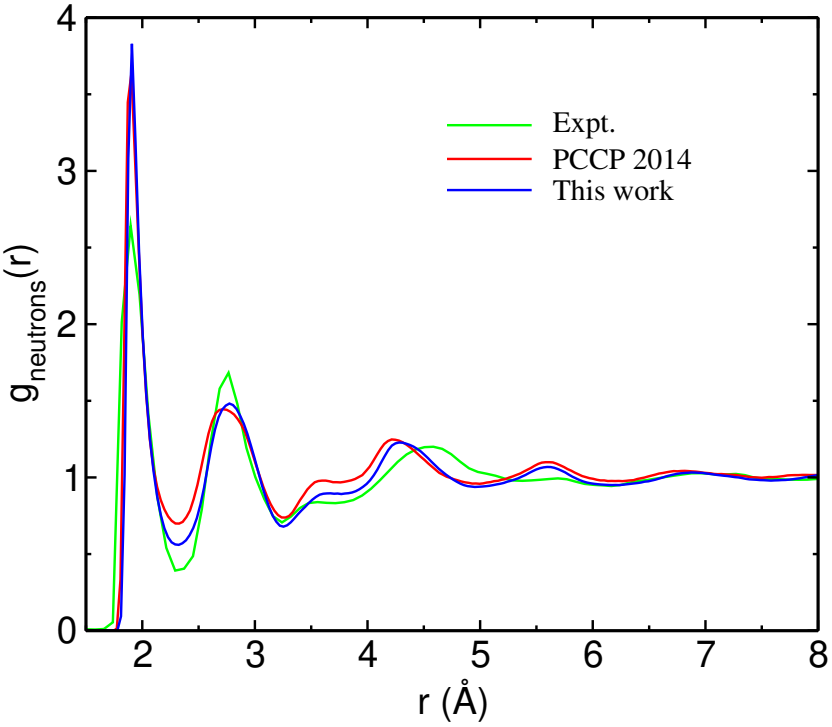

Figure 2. Neutrons total pair correlation function of the obtained glassy TeO_2 models compared to experiments from Ref. [27].

4. Conclusions

In summary, we provide a new parametrization of the core-shell Buckingham potential of Te-O oxides. Our parametrization allows one to accurately reproduce the structures of crystalline phases of α-, β-, and γ-TeO_2 and its transferability was tested against a large family of Te-O based oxides showing a good accuracy. We then took advantage of the new parametrization to generate a high temperature model of TeO_2 and find that it features a liquid like dynamical

behaviour. In addition, we showed that amorphous TeO_2 could be obtained by quenching from the melt and features a very good agreement with experiments, while slightly improving upon previously published models. Overall, we are convinced that the present parametrization will be a valuable tool to tackle the study of complex Te-O based glassy systems.

Acknowledgments

We used computational resources provided by the computing facilities MCIA (Mésocentre de Calcul Intensif Aquitain) of the Université de Bordeaux and of the Université de Pau et des Pays l'Adour.

References

[1] Rivera V A G and Manzani D (eds) 2017 *Technological Advances in Tellurite Glasses: Properties, Processing, and Applications* Springer Series in Materials Science (Springer International Publishing) ISBN 978-3-319-53036-9

[2] Barbosa L C, Filho C O and Chillcce E F 2017 Photonic Applications of Tellurite Glasses *Technological Advances in Tellurite Glasses: Properties, Processing, and Applications* Springer Series in Materials Science (Cham: Springer International Publishing) pp 93–100 ISBN 978-3-319-53038-3

[3] El-Mallawany R A H 2014 *Tellurite Glasses Handbook: Physical Properties and Data* (CRC Press) ISBN 978-1-4200-4208-5

[4] Jeansannetas B, Blanchandin S, Thomas P, Marchet P, Champarnaud-Mesjard J, Merle-Mjean T, Frit B, Nazabal V, Fargin E, Le Flem G, Martin M, Bousquet B, Canioni L, Le Boiteux S, Segonds P and Sarger L 1999 *J. Solid State Chem.* **146** 329–335 ISSN 00224596

[5] Stegeman R, Jankovic L, Kim H, Rivero C, Stegeman G, Richardson K, Delfyett P, Guo Y, Schulte A and Cardinal T 2003 *Optics Letters* **28** 1126–1128 ISSN 1539-4794

[6] Suzuki T, Shiosaka T W, Miyoshi S and Ohishi Y 2011 *Journal of Non-Crystalline Solids* **357** 2702–2707 ISSN 0022-3093

[7] Shi-An Z, Zhen-Rong S, Xi-Hua Y, Zu-Geng W, Jian L and Wen-Hai H 2005 *Chinese Physics* **14** 1578–1580 ISSN 1009-1963, 1741-4199

[8] Gao W, Liao M, Kawashima H, Cheng T, Suzuki T and Ohishi Y 2012 *Japanese Journal of Applied Physics* **51** 122702 ISSN 0021-4922, 1347-4065

[9] Brady G W 1957 *The Journal of Chemical Physics* **27** 300–303 ISSN 0021-9606

[10] Dimitriev Y, Dimitrov V, Bart J C J and Arnaudov M 1981 *Zeitschrift für anorganische und allgemeine Chemie* **479** 229–240 ISSN 1521-3749

[11] McLaughlin J C, Tagg S L and Zwanziger J W 2001 *The Journal of Physical Chemistry B* **105** 67–75 ISSN 1520-6106

[12] Niida H, Uchino T, Jin J, Kim S H, Fukunaga T and Yoko T *The Journal of Chemical Physics* **114** 459–467 ISSN 0021-9606

[13] Sakida S, Hayakawa S and Yoko T 1999 *Journal of Non-Crystalline Solids* **243** 1–12 ISSN 0022-3093

[14] Sakida S, Hayakawa S and Yoko T 1999 *Journal of Non-Crystalline Solids* **243** 13–25 ISSN 0022-3093

[15] McLaughlin J C, Tagg S L, Zwanziger J W, Haeffner D R and Shastri S D 2000 *Journal of Non-Crystalline Solids* **274** 1–8 ISSN 0022-3093

[16] Osaka A, Jianrong Q, Nanba T, Takada J, Miura Y and Yao T 1992 *Journal of Non-Crystalline Solids* **142** 81–86 ISSN 0022-3093

[17] Tatsumisago M, Lee S K, Minami T and Kowada Y 1994 *Journal of Non-Crystalline Solids* **177** 154–163 ISSN 0022-3093

[18] Noguera O, Merle-Méjean T, Mirgorodsky A, Smirnov M, Thomas P and Champarnaud-Mesjard J C 2003 *Journal of Non-Crystalline Solids* **330** 50–60 ISSN 00223093

[19] Kalampounias A G, Yannopoulos S N and Papatheodorou G N 2007 *Journal of Physics and Chemistry of Solids* **68** 1035–1039 ISSN 0022-3697
[20] Kalampounias A G, Papatheodorou G N and Yannopoulos S N 2007 *Journal of Physics and Chemistry of Solids* **68** 1029–1034 ISSN 0022-3697
[21] Zaki M R, Hamani D, Dutreilh-Colas M, Duclère J R, Masson O and Thomas P 2018 *Journal of Non-Crystalline Solids* **484** 139–148 ISSN 0022-3093
[22] Zaki M R, Hamani D, Dutreilh-Colas M, Duclère J R, de Clermont-Gallerande J, Hayakawa T, Masson O and Thomas P 2019 *Journal of Non-Crystalline Solids* **512** 161–173 ISSN 0022-3093
[23] Noguera O, Smirnov M, Mirgorodsky A P, Merle-Méjean T, Thomas P and Champarnaud-Mesjard J C 2004 *Journal of Non-Crystalline Solids* **345-346** 734–737 ISSN 0022-3093
[24] Uchino T and Yoko T 1996 *Journal of Non-Crystalline Solids* **204** 243–252 ISSN 0022-3093
[25] Pietrucci F, Caravati S and Bernasconi M 2008 *Physical Review B* **78** 064203
[26] Kalampounias A G, Tsilomelekis G and Boghosian S 2015 *The Journal of Chemical Physics* **142** 154503 ISSN 0021-9606, 1089-7690
[27] Gulenko A, Masson O, Berghout A, Hamani D and Thomas P 2014 *Phys. Chem. Chem. Phys.* **16** 14150–14160 ISSN 1463-9084
[28] Thomas P A 1988 *J. Phys. C: Solid State Phys.* **21** 4611–4627 ISSN 0022-3719
[29] Beyer H 1967 *Cryst. Mat.* **124** 228 – 237
[30] Champarnaud-Mesjard J C, Blanchandin S, Thomas P, Mirgorodsky A, Merle-Mejean T and Frit B 2000 *J. Phys. Chem. Solids* **61** 1499–1507
[31] Gale J D and Rohl A L 2003 *Mol. Sim.* **29** 291–341 ISSN 0892-7022
[32] Klein W, Curda J, Peters E M and Jansen M 2005 *Zeitschrift für anorganische und allgemeine Chemie* **631** 2893–2899 ISSN 0044-2313, 1521-3749
[33] Koçak M, Platte C and Trömel M 1979 *Acta Crystallographica Section B Structural Crystallography and Crystal Chemistry* **35** 1439–1441 ISSN 0567-7408
[34] Rossell H, Leblanc M, Ferey G, Bevan D, Simpson D and Taylor M 1992 *Australian Journal of Chemistry* **45** 1415 ISSN 0004-9425
[35] Weil M and Stöger B 2008 *Acta Crystallographica Section C Crystal Structure Communications* **64** i79–i81 ISSN 0108-2701
[36] Trömel V M and Scheller T 1976 *Zeitschrift für anorganische und allgemeine Chemie* **427** 229–234 ISSN 00442313
[37] Daniel F, Moret J, Maurin M and Philippot E 1978 *Acta Crystallographica Section B Structural Crystallography and Crystal Chemistry* **34** 1782–1786 ISSN 0567-7408
[38] Folger F 1975 *Zeitschrift f?r anorganische und allgemeine Chemie* **411** 103–110 ISSN 0044-2313, 1521-3749
[39] Weil M 2005 *Acta Crystallographica Section E Structure Reports Online* **61** i237–i239 ISSN 1600-5368
[40] Tagg S L, Huffman J C and Zwanziger J W 1994 *Chemistry of Materials* **6** 1884–1889 ISSN 0897-4756, 1520-5002
[41] Masse R, Guitel J and Tordjman I 1980 *Materials Research Bulletin* **15** 431–436 ISSN 00255408
[42] Platte C and Trömel M 1981 *Acta Crystallographica Section B Structural Crystallography and Crystal Chemistry* **37** 1276–1278 ISSN 05677408
[43] Mayer H and Weil M 2003 *Zeitschrift f?r anorganische und allgemeine Chemie* **629** 1068–1072 ISSN 0044-2313, 1521-3749
[44] Barrier N, Malo S, Hernandez O, Hervieu M and Raveau B 2006 *Journal of Solid State Chemistry* **179** 3484–3488 ISSN 00224596
[45] Todorov I T, Smith W, Trachenko K and Dove M T 2006 *J. Mat. Chem.* **16** 1911–1918 ISSN 1364-5501